Since January 2020 Elsevier has created a COVID-19 resource centre with free information in English and Mandarin on the novel coronavirus COVID-19. The COVID-19 resource centre is hosted on Elsevier Connect, the company's public news and information website.

Virus Research 253 (2018) 1–11

Contents lists available at ScienceDirect

Virus Research

journal homepage: www.elsevier.com/locate/virusres

Porcine epidemic diarrhea virus through p53-dependent pathway causes cell cycle arrest in the G0/G1 phase

Pei Sun[a,1], Haoyang Wu[a,1], Jiali Huang[b], Ying Xu[b], Feng Yang[b], Qi Zhang[b], Xingang Xu[b,*]

[a] College of Animal Science and Technology, Anhui Agricultural University, Hefei, Anhui, 230036, China
[b] College of Veterinary Medicine, Northwest A&F University, Yangling, Shaanxi, 712100, China

ARTICLE INFO

Keywords:
PEDV
Cell cycle arrest
p53 pathway
Virus replication

ABSTRACT

Porcine epidemic diarrhea virus (PEDV), an enteropathogenic *Alphacoronavirus*, has caused enormous economic losses in the swine industry. p53 protein exists in a wide variety of animal cells, which is involved in cell cycle regulation, apoptosis, cell differentiation and other biological functions. In this study, we investigated the effects of PEDV infection on the cell cycle of Vero cells and p53 activation. The results demonstrated that PEDV infection induces cell cycle arrest at G0/G1 phase in Vero cells, while UV-inactivated PEDV does not cause cell cycle arrest. PEDV infection up-regulates the levels of p21, cdc2, cdk2, cdk4, Cyclin A protein and down-regulates Cyclin E protein. Further research results showed that inhibition of p53 signaling pathway can reverse the cell cycle arrest in G0/G1 phase induced by PEDV infection and cancel out the up-regulation of p21 and corresponding Cyclin/cdk mentioned above. In addition, PEDV infection of the cells synchronized in various stages of cell cycle showed that viral subgenomic RNA and virus titer were higher in the cells released from G0/G1 phase synchronized cells than that in the cells released from the G1/S phase and G2/M phase synchronized or asynchronous cells after 18 h p.i.. This is the first report to demonstrate that the p53-dependent pathway plays an important role in PEDV induced cell cycle arrest and beneficially contributes to viral infection.

1. Introduction

Viral infection disrupts cell cycle by inducing activation of a series of signal transduction pathways, which play an important role in viral life cycle by promoting replication of progeny viruses after viral infection (Davy and Doorbar, 2007). Examples can be found among DNA viruses, retroviruses, and RNA viruses. For example, the cell proliferation induced by Reovirus δ1 s nonstructural protein is blocked in the G2/M phase cell cycle (Poggioli et al., 2000); Influenza A virus A/WSN/33 (H1N1) causes cell cycle arrest in G0/G1 phase, which is beneficial to the expression of viral protein and generation of progeny virus (He et al., 2010); In the coronavirus family, mouse hepatitis virus (MHV) replication and some severe acute respiratory syndrome coronavirus (SARS-CoV) proteins are able to induce cell cycle arrest at G0/G1 phase (Chen and Makino, 2004; Yuan et al., 2005; Yuan et al., 2006; Yuan et al., 2007); Infectious bronchitis virus (IBV) infection causes cell arrest in G2/M phase to favor viral replication (Dove et al., 2006); Transmissible gastroenteritis virus (TGEV) infection induces cell cycle arrest at S and G2/M phases (Ding et al., 2013); PEDV M protein and ORF3 protein can block S-phase progression in mammalian cells (Xu et al., 2015; Ye et al., 2015); However, the effects of PEDV infection on the cell cycle in Vero cells and the significance of PEDV replication in cell cycle regulation remains to be further studied.

The cell cycle can be divided into a number of separate events (Pines, 1999): DNA replication (S phase), nuclear division (mitosis [M]), and cell division (cytokinesis), separated by two gap periods (G1 and G2). Quiescent cells are described as being in G0. Progression in each phase of the cycle and from one phase to the next is tightly regulated and highly orchestrated, controlled by cyclins and cyclin-dependent kinases as well as other factors. In the G1 phase, cells express three kinds of Cyclin D (cyclin D1, D2 and D3), combining with and activating cdk4/6, which is necessary for cells to enter the G1 phase from G0 phase (Besson et al., 2008). Cyclin E is also expressed in the G1 phase, which combines with cdk2 to make the cells complete the G1/S phase transition. The forward progression of S phase requires the kinase complex formed by cyclin A and cdk2 (Duronio, 2012). At the late stage of G2 and early M, the combination of Cyclin A and cdk1 (cdc2) initiate cells into M phase (Enomoto et al., 2009). It has been shown that these cell cycle regulatory molecules are regulated by some upstream pathways, such as p53 signaling. p53 monitors genome integrity during cell

* Corresponding author.
E-mail address: tiger2003@nwsuaf.edu.cn (X. Xu).
[1] Both two authors contributed equally to this work.

https://doi.org/10.1016/j.virusres.2018.05.019
Received 17 March 2018; Received in revised form 17 May 2018; Accepted 21 May 2018
Available online 22 May 2018
0168-1702/

cycle G1/S and G2/M. If cell DNA is damaged, the cells are arrested in the G1 phase and cannot enter the S phase, or the cells are stagnated in the G2 phase and cannot enter the M phase, p53 is able to bind to the damaged DNA and promote its Repair (Schlereth et al., 2010). p21 is the down-stream signaling molecule of tumor suppressor gene p53, because the promoter of p21 gene contains p53 binding domain, so p53 can activate p21 gene by transcription (Roy et al., 2009). p21 can extensively act on cdk-Cyclin complexes and inhibit their activity, especially G1 phase cdk4/6-Cyclin D complexes (Starostina and Kipreos, 2011). In the present study, we investigated the effects of PEDV replication on the cell cycle progression, the roles of p53 signaling activation in regulation of cell cycle progression in PEDV-infected cells, and the significance of cell cycle regulation in PEDV replication. The results showed that PEDV infection may affect the cell cycle and promote replication of viral genes.

2. Materials and methods

2.1. Viruses, cells and antibodies

Vero cells (ATCC, CCL-33) were grown in Dulbecco Minimal Essential Medium (D-MEM) (Gibco BRL, MD, US) supplemented with 10% heat-inactivated fetal bovine serum (PAN), 1% penicillin/streptomycin (Invitrogen) at 37℃ in 5% CO_2 atmosphere incubator. In the present study, the CH/SXYL/2016 strain of PEDV (GenBank accession number is MF462814) was isolated from intestinal tract contents of PEDV infected piglets in Shaanxi province in China. 0.5 MOI PEDV (containing 10 μg/ml trypsin) infection solution was incubated for 1 h, then the virus was removed and washed 3 times with PBS, then DMEM containing 2% FBS was added, and cell samples were taken at the indicated time points for detection. Viral titers were determined by median tissue culture infectious dose($TCID_{50}$) (Reed and Muench, 1938).

Antibodies against cdc2, cdk2, cdk4, cdk6, Cyclin B1, Cyclin D1, Phospho-p53 (Ser15 and Ser20), p21 Waf1/Cip1 and β-Actin were purchased from Cell Signaling Technology. Antibodies against Cyclin A, Cyclin E, p53 were purchased from Santa Cruz. Horseradish peroxidase (HRP)-conjugated anti-mouse IgG and anti-rabbit IgG were purchased from Bioss. FITC-conjugated antirabbit IgG was purchased from Molecular Probes.

2.2. Measurement of cell proliferation and viability

MTT assay was carried out using the cell proliferation kitI(MTT) according to the manufacturer's recommended procedures (Roche Applied Science). Briefly, Vero cells plated in 96-well plates at approximately 90% confluence were infected with PEDV at an MOI of 0.5, 1.0, 2.0, 5.0, 10.0. At various times postinfection, 20 μl of MTT labeling reagent was added to each well and incubated at 37℃ for 4 h. After 150 μl of solubilization solution was added, the absorbance was measured at 550 nm in an enzyme-linked immunosorbent assay reader.

2.3. BrdU incorporation and flow cytometry analysis

2×10^6 PEDV-infected Vero cells were treated with a concentration of 10 μm bromodeoxyuridine (BrdU) (Sigma), incubated at 37℃ for 30 min to allow BrdU incorporation, rinsed with phosphate-buffered saline (PBS) twice and added with 2 ml EDTA/trypsin at 37℃ for 1 min. Vero cells were pelleted by centrifugation at 1000 × g for 5 min and then fixed in 1 ml of 75% ethanol for 4 h at 4℃. BrdU-labeled cell samples in 75% ethanol solution were pelleted by centrifugation at 1500 × g for 5 min, rinsed with 1 ml PBS, and then incubated in 1 ml of 0.1 M HCl in PBS at 37℃ for 10 min before addition of 3 ml PBS. Samples were then pelleted by centrifugation at 1000 × g for 5 min before addition of 100 μl anti-BrdU solution (anti-BrdU antibody [BD Biosciences] diluted 1:5 in PBS, 0.5% Tween 20, and 1% FBS) and incubated for 60 min at 25℃. Samples were rinsed with PBS twice, pelleted by centrifugation at 1000 × g for 5 min before addition of 100 μl anti-mouse fluorescein isothiocyanate (FITC)-labeled solution (antibody diluted 1:10 in PBS, 0.5% Tween 20, and 1% FBS) and incubated for 30 min in the dark at 25℃. Samples were rinsed twice in PBS before addition of 1 ml of PI staining solution (PBS, 50 μg/ml PI, 20 μg/ml RNase A). Labeled cells were analyzed for PI staining and BrdU incorporation using a FACSCalibur analyzer (Becton Dickinson), and percentages of cells in the G0/G1, S, and G2/M phases in each sample were determined by gating using CellQuest software (Becton Dickinson).

2.4. G0/G1, G1/S, and G2/M synchronization in Vero cells

Vero cells were synchronized at G0/G1 phase using FBS-free DMEM medium treatment. Vero cells were cultivated for 48 h using DMEM medium without FBS supplementation. Synchronized cells were mock infected or infected with 0.5 MOI of PEDV. After virus adsorption for 1 h and PBS rinse, cells were treated with medium and harvested at different times for RT-qPCR and flow cytometric analysis.

Vero cells were synchronized at G1/S phase using double-thymidine method. Vero cells were cultivated with DMEM medium containing 2 mM thymidine (Sigma) for 16 h, then rinsed with PBS for three times. After maintained for 12 h, cells were treated as described above once again and infected with 0.5 MOI of PEDV eventually. At 18 h post infection (p.i.), cells were harvested for RT-qPCR and flow cytometric analysis.

Vero cells were synchronized at G2/M phase using nocodazole (Sigma) treatment. Cells were treated with DMEM medium containing 60 ng/ml thymidine (Sigma) for 16 h, then rinsed with PBS for three times and infected with 0.5 MOI of PEDV eventually. At 18 h p.i., cells were harvested for RT-qPCR and flow cytometric analysis.

2.5. Western blot analysis

Cells in the experimental group were harvested and treated with RIPA Buffer (Sigma). Protein concentrations were determined using the BCA Protein Assay Kit. Equal amounts of proteins were transfer to polyvinylidene difluoride (PVDF) membrane (Millipore Corp, Atlanta, GA, US) by 12% SDS-PAGE followed by wet-transfer cell (Bio-Rad, Trans-blot SD). The membranes were blocked with 2.5% nonfat dry milk in PBS'T (0.5% Tween-20 in PBS) at room temperature for 1 h and then membranes were probed with primary antibodies over night at 4℃, followed by HRP-conjugated secondary antibodies incubation at room temperature for 1 h. Western blotting was performed using enhanced chemiluminescence ECL (Pierce, Rockford, IL, US) as described in the manufacturer's instructions.

2.6. RNA analysis by real-time quantitative PCR (RT-qPCR)

Total RNAs were extracted from the PEDV-infected Vero cell by using the RNeasy mini kit (Qiagen, Valencia, CA) according to manufacturer's instructions. RNA concentrations for all samples were determined, and equal amounts of 1 μg RNA for each sample went through reverse transcription (RT) using the High-Capacity cDNA Reverse Transcription kit (Applied Biosystems, Carlsbad, CA) according to the manufacturer's instructions. Real-time quantitative RT-PCR was performed using the SYBR Green PCR Master Mix (Applied Biosystems) in an TL988-IV Real Time PCR Thermocycler. The primers for RT-qPCR in this study were described in Table 1. The real-time PCR was carried out in a final volume of 10 μl, sense and anti-sense primers (0.4 μmol/l) and target cDNA (4 ng). The reaction consists of a 10 min initialization at 95℃ and 35 cycles of 3s-denaturation at 95℃, 15s-annealing & elongation at 60℃. A negative control was included in each run and the specificity of amplification reaction was checked by melting curve (Tm value) analysis. Genomic equivalent normalization of each sample was

Table 1
The primers for real-time RT-qPCR.

Gene	Forward primer (5'-3')	Reverse primer (5'-3')	Product (bp)	Density (μM)	Accession no.
N	TGAGGGTGTTTTCTGGGTTG	TTGCCATTGCCACGACTC	192	10	AF353511.1
M	TTGGTGGTCTTTCAATCCTG	CTGAGTAGTCGCCGTGTTTT	299	10	KJ960180
ORF3	GCAGGCTTTGTTTAGTCTGCTT	TGCCAAAAGTGATGTAATGGTC	162	10	KU9775001
P53	TCCATTTGCTTTGTCCCG	TGGCTGATTGTAAACTAACCCT	177	10	AH007665.2
P21	GTGGCAGTAGAGGCTATGGA	TAGGTGGAGAAACGGGAAC	223	10	NM_001291549.1
PCNA	CCATATTGGAGATGCTGTTG	TGAGTGTCACCGTTGAAGAG	227	10	NM_002592.2
β-actin	GGACTTCGAGCAGGAGATGG	AGGAAGGAGGGCTGGAAGAG	138	10	XM_003124280.1

performed using the corresponding CT values of the porcine β-actin housekeeping gene. The relative quantification of gene expression was analyzed by the $2^{-\Delta\Delta CT}$ Method (Livak and Schmittgen, 2001).

2.7. Inhibitor treatments

Pifithrin-α (PFT-α) purchased from Sigma and stored as a 10 mM stock solution in DMSO. In order to reduce the activation of p53, PFT-α (10 μM) was diluted in DMEM and added to the culture medium cultivated for an hour before infection. Inhibitor was not included in the virus inoculum. After an hour of PEDV adsorption, the virus inoculum was removed and the fresh basal medium containing inhibitors was added to the culture medium. At the indicated time, the cells were collected and the related indexes were detected.

2.8. Confocal microscopy

Mock-infected and PEDV-infected (MOI of 0.5) Vero cells were fixed at 0, 12, 24 h p.i., and confocal sections were captured on an LECIA TCS SP8 microscope (Leica Microsystems). PEDV-infected cells were labeled with an anti-PEDV polyclonal sera (1:200) and detected with donkey anti-mouse FITC (1:300) (green). Nuclei were stained with Hoechst 33342 (blue).

2.9. Statistical analysis

All data were mean ± SEM of three independent experiments in triplicate. Results were analyzed by one-way analysis of variance (ANOVA). For each assay, using student's *t*-test to statistical comparison. A value of $P < 0.05$ was considered significant.

3. Results

3.1. Inhibition of cell proliferation by PEDV infection of Vero cells

Cell proliferation analysis showed that after 30 h p.i., a slight inhibitory effect on cell growth activity was observed in cells infected with 0.5 MOI of PEDV (Fig. 1), but there was no significant difference compared with the control group. With the prolongation of virus infection time, cell viability decreased gradually, which was significantly different at 36 h compared with the control group. After 24 h p.i. with 1 or more MOI of PEDV, the cell growth activities were significantly inhibited (Fig. 1), indicating that PEDV inhibited Vero cells growth in an MOI- and time-dependent manner. To reduce the experimental error, a 0.5-MOI virus infection within 24 h was chosen to complete this experiment.

3.2. Confocal microscopy

PEDV laboratory strains cause prominent cell fusion in infected cell cultures, it is unlikely that the cell cycle could progress properly in fused cells. It has been reported that syncytia induction led to transient activation of cdk1/cyclin B, followed by a rapid decrease in cyclin B

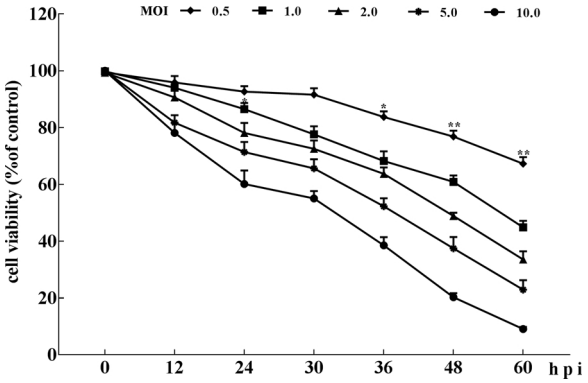

Fig. 1. Analysis of cell proliferation by MTT assay. Vero cells at 90% confluence in 96-well plates were mock- or PEDV-infected at an MOI of 0.5, 1.0, 2.0, 5.0, 10.0. At various times post-infection, MTT assays were performed. Data are presented as percentage of live cells compared with that of mock-infected cells at 0, 12, 24, 30, 36, 48 and 60 h p.i.. The percentages are results of three repeated experiments. $^*P < 0.05$, $^{**}P < 0.01$ versus mock infection.

levels, to cause the cell-cycle arrest (Castedo et al., 2004). To determine whether syncytia production occurred within 24 h of infection with 0.5 MOI PEDV, we used Confocal microscopy to detect PEDV infection 0, 12, 24 h p.i. Results showed no syncytia production within 24 h of PEDV infection (Fig. 2).

3.3. PEDV-infected cells accumulate at G0/G1 of the cell cycle

To investigate the effect of PEDV infection on cell cycle progression, Mock- or PEDV-infected Vero cells were harvested at different time, and the cell cycle distribution was detected by flow cytometry. Representative cell cycle histograms and profiles in Vero cells were presented in Fig. 3 respectively. In PEDV-infected Vero cells, there was a significant increase in the proportion of cells in the G0/G1 phase of the cell cycle from 6 h p.i., which continued to increase with the lastingness of infection compared to mock-infected cells (Fig. 3). The results showed that the infection of PEDV induced cell cycle arrest at G0/G1 phase.

In PEDV-infected cells, PEDV infectious levels were evaluated by detection of the sgmRNAs (N sgmRNA, ORF3 sgmRNA, M sgmRNA) of PEDV using RT-qPCR. The sgmRNA levels of N, M and ORF3 could be detected after 6 h p.i.. The results showed that the levels of PEDV sgmRNA increased significantly from 12 h p.i. to 24 h p.i. in PEDV-infected Vero cells (Fig. 4A). In addition, the virus titers were determined at different times after inoculation. The results showed that the virus titer showed a rapid increase after infection 12 h p.i. (Fig. 4B).

In order to further determine whether the PEDV-induced G0/G1 arrest requires virus replication, UV-inactivated PEDV was inoculated in Vero cells, and cell cycle profiles were measured at 18 h p.i. by flow cytometry. The results showed that a significant G0/G1 arrest was detectable only in cells infected with intact virus, not in mock-infected cells or cells infected with UV-treated virus (Fig. 4C), suggesting that

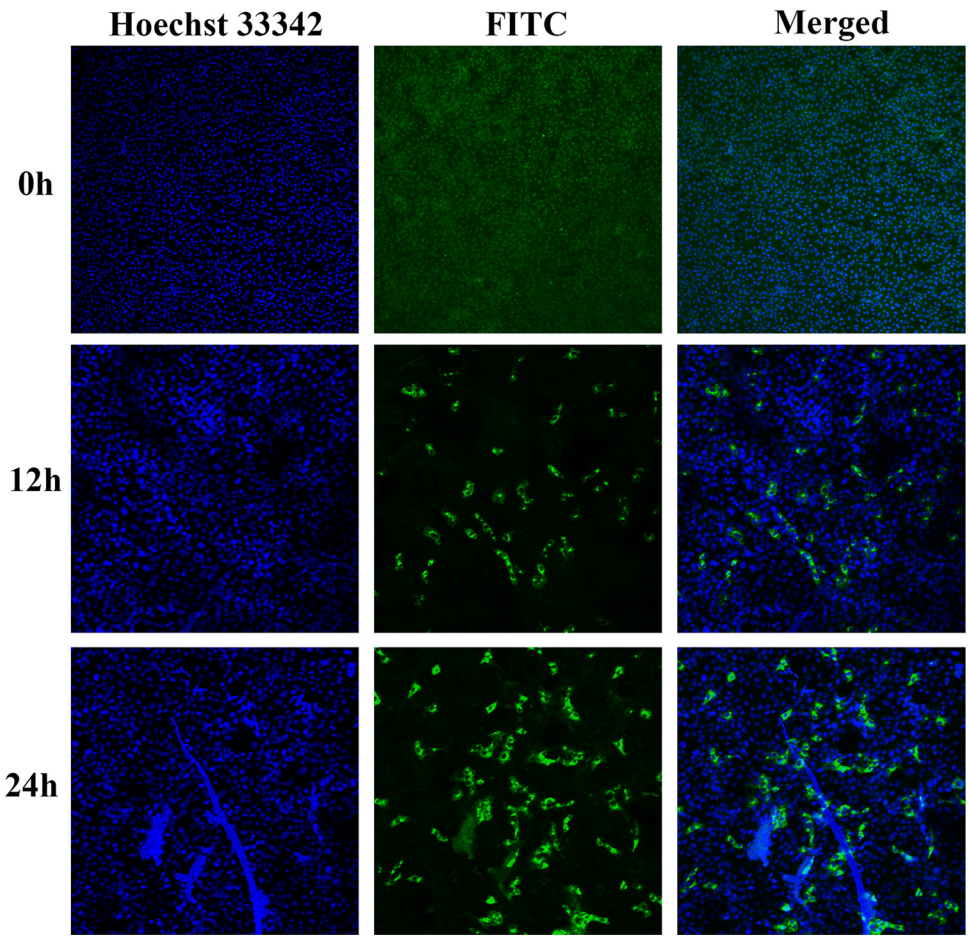

Fig. 2. Vero cells were infected with PEDV and imaged using confocal microscopy. Vero cells were mock infected or infected with PEDV at an MOI of 0.5. At the indicated times, cells were co-stained with antibody, FITC and Hoechst 33342 analyzed for Confocal microscopy. Viral proteins were labeled with the appropriate antibody and FITC and are shown in green, Nuclei were stained with Hoechst 33342 (blue), and the two images were superimposed. Magnification of all images is ×100 (For interpretation of the references to colour in this figure legend, the reader is referred to the web version of this article).

viral replication induces cell cycle arrest in PEDV-infection cells.

3.4. PEDV infection of quiescent cells induces cell cycle arrest

To further confirm that PEDV replication caused G0/G1 phase cell cycle arrest, we infected serum-starved quiescent cells with PEDV and examined cell cycle progression after serum stimulation. As shown in Fig. 5, prior to PEDV infection, 82.2% of serum-starved Vero cells were successfully blocked in G0/G1 phase, after infection, much more dramatic increases (5%–15%) of G0/G1-phase cells were observed in 0.5 MOI PEDV-infected cells at the same time points compared with the mock-infected cells. Also similar phenomena were seen in asynchronous Vero cells. In addition, the virus titers were determined at different times after inoculation. The results showed that the virus titer showed a rapid increase after infection 12 h p.i. (Fig. 4B)

3.5. cdc2, cdk2, cdk4, Cyclins A increased and Cyclins E decreased in PEDV-infected cells

As progression through the cell cycle is mediated by cdks complexed with corresponding Cyclins, the possibility that PEDV infection would modulate such cell cycle regulators at the protein level was investigated. Western blot analysis of various cdks and cyclins were carried out in PEDV-infected Vero cells. We detected related levels of cell cycle regulators at 0, 6, 12, 18 and 24 h p.i. in PEDV-infected cells. The results showed that the cdc2, cdk2, cdk4 and Cyclin A levels of PEDV-infected cells were higher than the ones of mock-infected cells at 6, 12, 18 and 24 h p.i. (Fig. 6). The Cyclin E levels began to decrease at 6 h p.i., compared to mock-infected cells, while cdk6, Cyclin D and Cyclin B1 did not show significant difference between mock-infected and PEDV-infected Vero cells (Fig. 6). These results indicated that PEDV infection could lead to an accumulation of cells in the G0/G1 phase through increasing and decreasing certain cell cycle factors that regulate the proceeding of G0/G1.

3.6. p53 and p21 mediated PEDV-induced cell cycle arrest

The levels of p53 and p21 were examined by Western blot analysis in 0.5 MOI PEDV-infected cells. The results showed that 0.5 MOI of PEDV increased the p53 level and induced its phosphorylation at serine 15 and 20 in Vero cells (Fig. 7A). Consequently, the level of p21 increased in PEDV infected Vero cells from 6 h p.i., and significantly increased at 12 h p.i. (Fig. 7A). Real-time RT-PCR analysis showed that the levels of p53 and p21 have the same increase trend as Western blot results, while proliferating-cell nuclear antigen (PCNA), which is involved in DNA replication within S phase, showed no obvious trend of change in PEDV-infected Vero cells (Fig. 7B). These results indicated that viral infection regulated the cell cycle by activating p53 to upregulate the expression of p21.

In order to further determine the roles of p53 in PEDV induced cell cycle arrest, p53 specific inhibitor PFT-α was used to block the p53 signaling pathway, which has no effect on the mRNA level and the titers of PEDV (Fig. 8A), cell cycle profiles and p21 expression, cdks and cyclins in PEDV-infected Vero cell. As shown in Fig. 8B, pre-incubation of PFT-α attenuated PEDV-induced G0/G1 phase arrest. In addition, Cyclin E expression increased, p21, cdc2, cdk2, cdk4 and Cyclin A expression decreased in PEDV-infected Vero cells with PFT-α compared to that with DMSO (Fig. 8C). These results indicated that p53 and p21 might play key roles in mediating PEDV-induced cell cycle arrest.

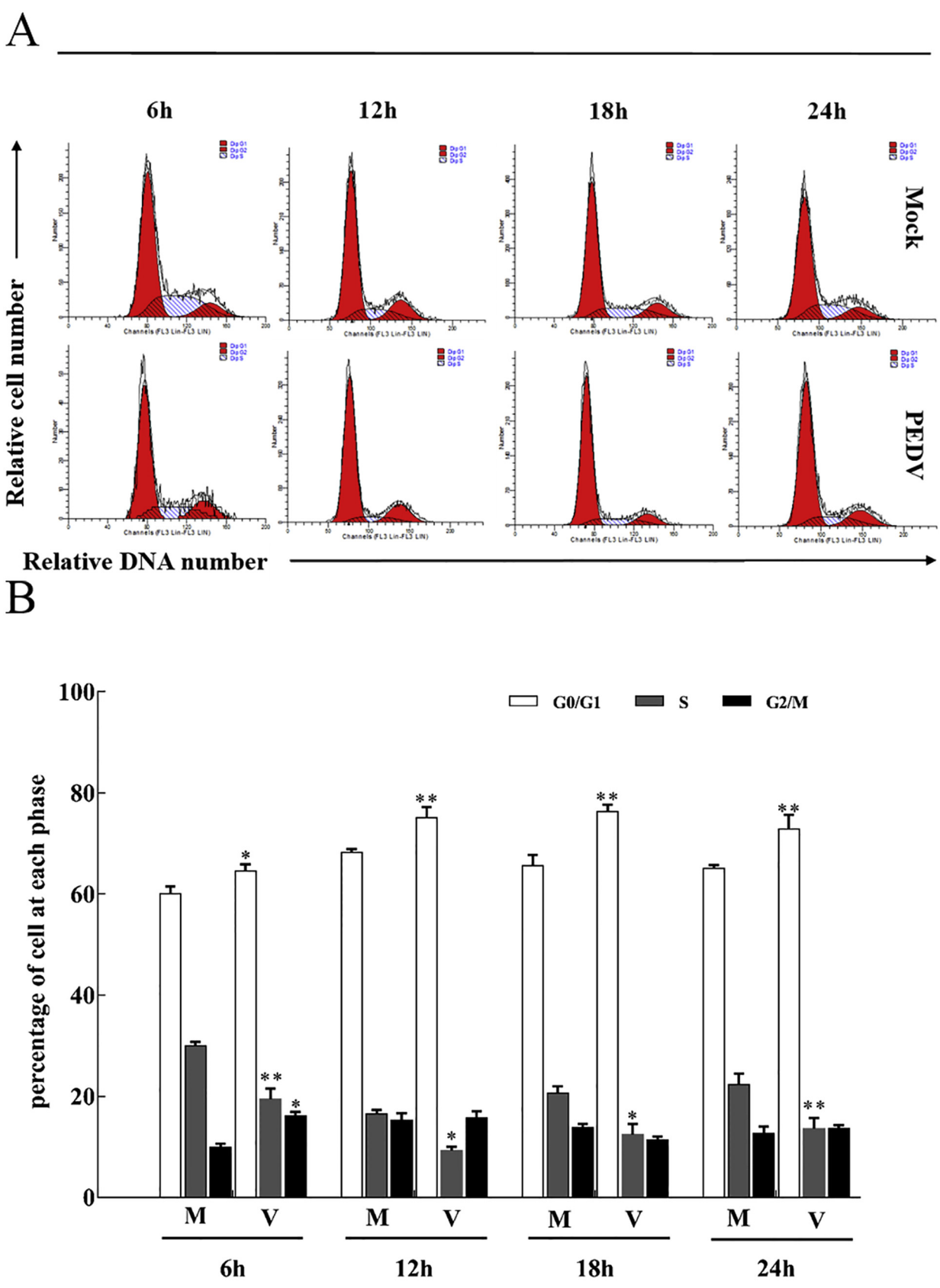

Fig. 3. Induction of aberrant cell cycle progression in PEDV-infected cells. Vero cells were mock infected or infected with PEDV at an MOI of 0.5. At the indicated times, cells were co-stained with BrdU and PI and analyzed for FACS analysis. The data are from one of three experiments. The histograms were analyzed using the GraphPad Prism 7.0 software to determine the percentage of cells at each phase of the cell cycle in Vero cells. The results are shown as mean ± SEM of three independent experiments. $^{*}P < 0.05$, $^{**}P < 0.01$ versus mock infection.

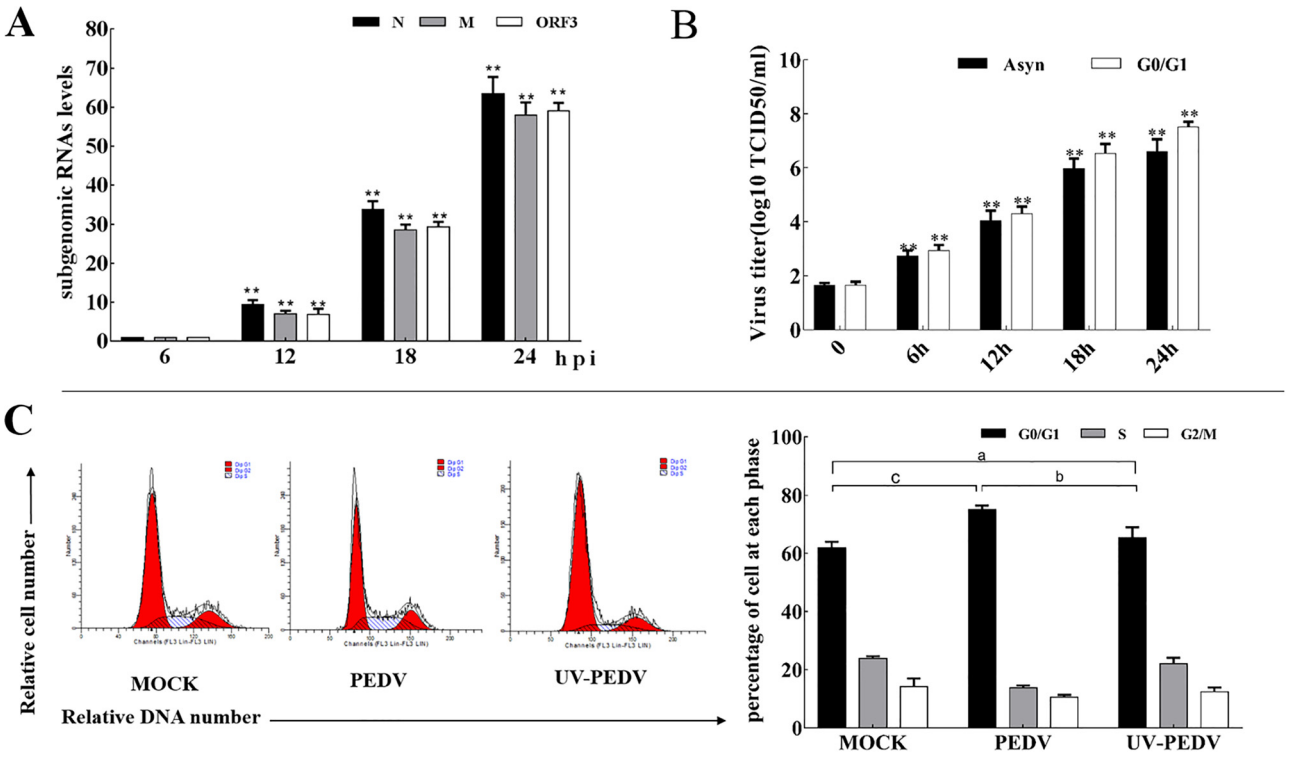

Fig. 4. PEDV-induced cell cycle arrest is dependent on PEDV replication. (A) Vero cells were mock infected or infected with 0.5 MOI of PEDV. At the indicated times, cells were collected and examined by RT-qPCR for PEDV sgmRNAs. The histograms were analyzed using the GraphPad Prism 7.0 software to determine PEDV sgmRNAs. Values are shown as the mean ± SEM of three independent experiments. $^{**}P < 0.01$ versus PEDV infected cells for 6 h. (B) Cells were treated as in (A), total virus at indicated times was harvested by freezing and thawing cells three times and the viral titers were shown as log10 $TCID_{50}$/ml. $^{**}P < 0.01$ versus PEDV infected cells for 0 h. (C) Cell cycle profiles were measured at 18 h p.i. by flow cytometry. The histograms were analyzed using the GraphPad Prism 7.0 software to determine the percentage of cells at each phase. The results are shown as mean ± SEM of three independent experiments. (a) $P > 0.05$ versus mock infection, (b) $P < 0.05$ versus UV-PEDV infection, (c) $P < 0.05$ versus mock infection.

3.7. Effects of cell cycle arrest at G0/G1 phase on PEDV replication

Our data indicated that PEDV caused an increase in the population of G0/G1 phase cells in virus-infected cells. In order to investigate the effect of synchroniz on PEDV replication in S phase and G2/M phase, synchronized cells in G0 phase, G1/S phase, G2/M phase and then either mock infected or infected with 0.5 MOI of PEDV, Vero cell cycle was determined by flow cytometry and PEDV sg mRNAs levels were detected using RT-qPCR at 18 h p.i.. Results showed that using serum deprivation treatments, over 80% of Vero cells were synchronized at the G0 phase (Fig. 9A). Using double-thymidine treatment, approximately 70% of cells were synchronized at the G1/S phase border in Vero cells (Fig. 9B). Using nocodazole treatments, over 75% of Vero cells were synchronized at the G2/M phase (Fig. 9C). In the cells released from the G0, G1/S, G2/M-phase-synchronized cells, the proportion of G0/G1 phase cells significantly increased in PEDV infected cells compared with mock infected cells at 18 h p.i. (Fig. 9).

Real-time RT-PCR analysis of the sg mRNAs of PEDV showed that the synthesis levels of sgmRNA (Fig. 10A) and the titers of the virus (Fig. 10B) were higher in the cells released from G0/G1 phase-synchronized cells than that in the cells released from G1/S or G2/M synchronized or asynchronous cells. These results further indicate that PEDV induced cell cycle arrest in the G0/G1 phase is beneficial to its own replication.

4. Discussion

Cell cycle regulation plays an important role in the cell infection of many viruses. PEDV cause prominent cell fusion in infected cell cultures, it is unlikely that the cell cycle could progress properly in fused cells, moreover syncytia induction the cell-cycle arrest (Castedo et al., 2004). In this study, we first confirmed that cells infected with 0.5 MOI PEDV for 24 h did not produce syncytia, and then investigated whether PEDV replication has an effect on Vero cell cycle progress. The results showed that PEDV replication induced cell cycle arrest in G0/G1 phase. To further confirm this cell cycle arrest, PEDV infection following serum starvation in which cells were synchronized in G0/G1 phase showed that cell cycle arrest was still in G0/G1 phase as the same result of asynchronous infection. Moreover, this accumulation depends on whether PEDV has the replication ability, since the UV-inactivated virus could not induce G0/G1 phase arrest.

Different viruses use different mechanisms to exploit or manipulate the cell cycle pathways of infected cells (Chowdhury et al., 2003; De Bolle et al., 2004; Li et al., 2007). cdk1, 2, 3, 4 and 6 are thought to be the major regulators of the core cycle, contributing to induction and/or progression at G1/S (cdk2, 4, 6), S (cdk2) and G2/M (cdk1) (Davidson and Niehrs, 2010). In G0 phase, pRb is nonphosphorylated but sequentially hypophosphorylated by Cyclin D-cdk4/6 complexes in early G1 and hyperphosphorylated by cyclin E-cdk2 complex in late G1 (Lundberg and Weinberg, 1998). A Cyclin E expression change can change Cyclin E-cdk2 activity and a cyclin D expression change can change Cyclin D-cdk4/6 activity, consequently altering the cell cycle transition from G0/G1 phase to S phase (Weinberg, 1995). In S phase, Cyclin A-cdk2 complex activity is required for S phase transition and DNA replication control (Elledge, 1996). In G2 phase, Cyclin B-cdk1 complex activity is associated with mitosis (Besson et al., 2008). In PEDV-infected cells, we observed significant increases of cdc2, cdk2, cdk4, Cyclin A and a decrease of Cyclin E involved in G0/G1 phase transition, consequently causing the G0/G1 phase arrest.

p53 modulation is a key event in various viruses' replication and the

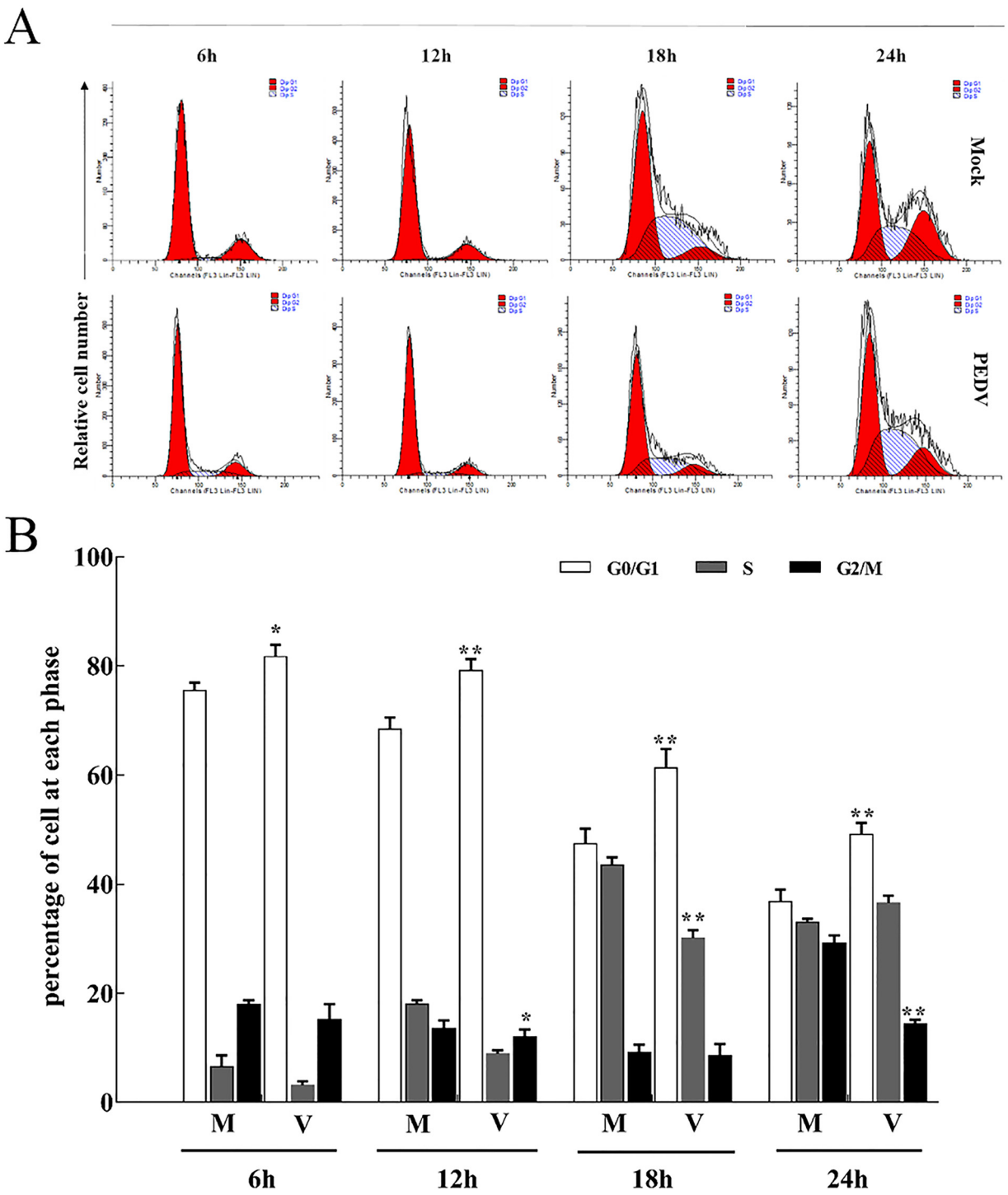

Fig. 5. PEDV infection induced quiescent Vero cells to accumulate in G0/G1 phase. Serum-starved Vero cells were mock infected or infected with 0.5 MOI of PEDV. After 1 h of virus adsorption, medium containing 10% FBS was added to the cells. At the indicated times, cells were co-stained with BrdU and PI and analyzed by FACS analysis. The data are from one of three experiments. The histograms were analyzed using the GraphPad Prism 7.0 software to determine the percentage of cells at each phase. The results are shown as mean ± SEM of three independent experiments. $^{*}P < 0.05$, $^{**}P < 0.01$ versus mock infection.

induction of cell cycle arrest in virus-infected cells, such as H1N1 and TGEV (He et al., 2010; Ding et al., 2013). But in this study, authors demonstrate that infection with coronavirus IBV induced cell cycle arrest was catalyzed by the modulation of various cell cycle regulatory genes and the accumulation of hypophosphorylated RB, but was independent of p53 (Li et al., 2007). The role of p53 as an antiviral target for coronavirus proteases to avoid innate immune response, such as PLP2, a catalytic domain of the nonstructural protein 3 of human coronavirus NL63 (HCoV-NL63), by promoting p53 degradation, PLP2 inhibits the p53-mediated antiviral response and apoptosis to ensure viral growth in infected cells (Yuan et al., 2015), SARS-CoV antagonize the viral inhibitor p53 via stabilizing CHY zinc-finger domain-containing 1 (RCHY1) and promoting RCHY1-mediated p53 degradation (Ma-Lauer et al., 2016). As a DNA damage response protein, p53 is involved in transcriptional activation of various genes involved in DNA repair and cell cycle arrest (Vogelstein et al., 2000), including p21 gene,

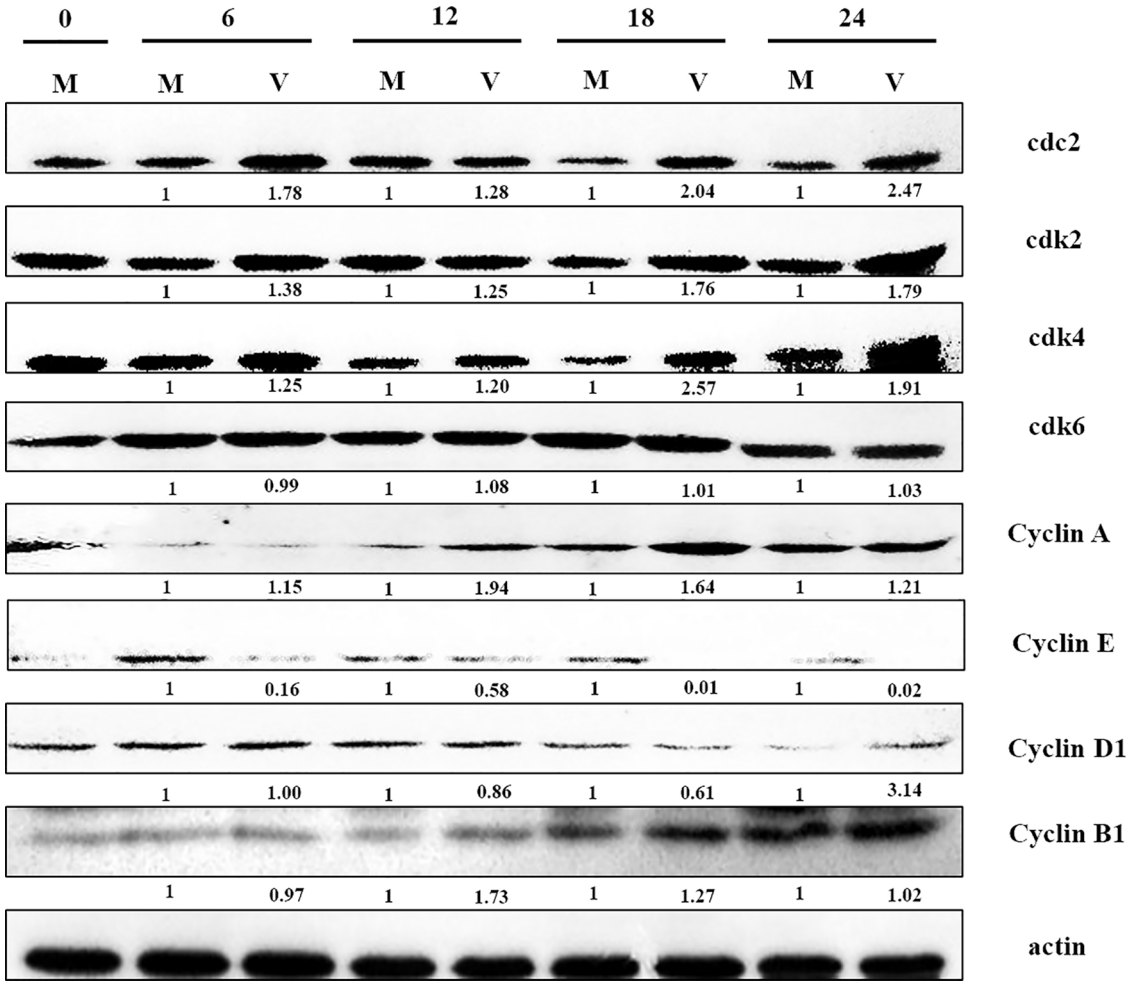

Fig. 6. Western blot analysis of total cellular protein isolated from mock (M) and 0.5 MOI PEDV-infected (V). Vero cells at 0, 6, 12, 18 and 24 h p.i. were lysed and equal amounts of proteins from the samples were tested by western blot analysis. The same membranes were also probed with β-actin as a loading control. The numbers below the proteins indicated the relative folds of mock infection after normalized to β-actin.

whose product is a cdk inhibitor that negatively suppresses the formation of the Cyclin E-cdk2 complex, which is important for G1/S transition. Thus, it is possible that PEDV-induced G0/G1 phase arrest is caused by p53 expression up-regulation and its downstream influence, including p21 expression alteration. In this study, Western blot and Real-time quantitative PCR showed that PEDV infection induced p53 and p21 accumulation and PCNA showed no significant change in mRNA levels. Furthermore, flow cytometry analysis showed PFT-α, a specific inhibitor of p53, prevented PEDV induced cell cycle arrest and the increases of p21, cdc2, cdk2, cdk4, Cyclin A as well as Cyclin E decrease. It's observed that PEDV-induced G0/G1 phase arrest in Vero cells virtually required the possible involvement of p53. It is known that

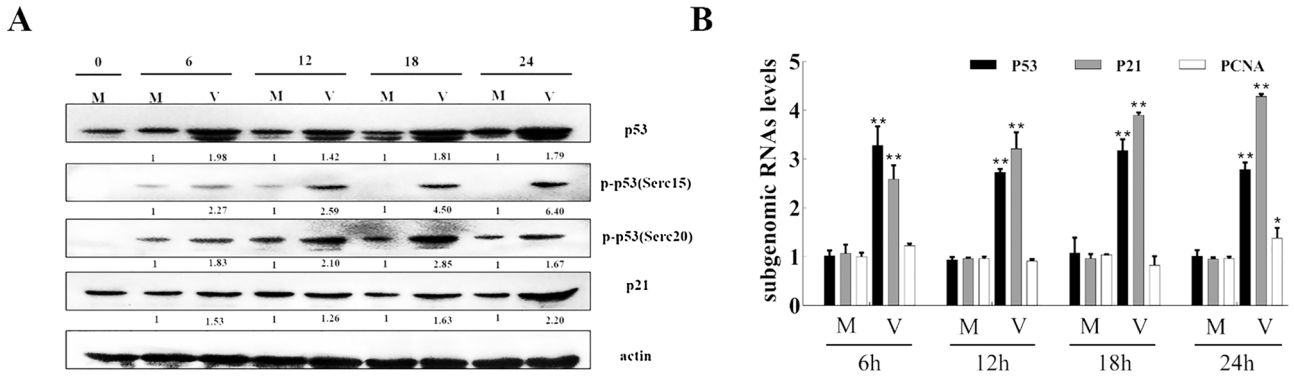

Fig. 7. Roles of p53 and p21 in PEDV-induced cell cycle arrest. (A) Vero cells were mock infected (M) or infected with 0.5 MOI of PEDV (V). Cells were collected at indicated times and subjected to western blot analysis. The numbers below the proteins indicate the relative folds of mock infection after normalized to β-actin. (B) Vero cells were mock infected or infected with 0.5 MOI of PEDV. At the indicated times, cells were collected and examined by RT-qPCR for p53, p21 and PCNA. The histograms were analyzed using the GraphPad Prism 7.0 software to determine gRNAs of p53, p21 and PCNA. Values are shown as the mean ± SEM of three independent experiments. $^{*}P < 0.05$, $^{**}P < 0.01$ versus PEDV infected cells for mock.

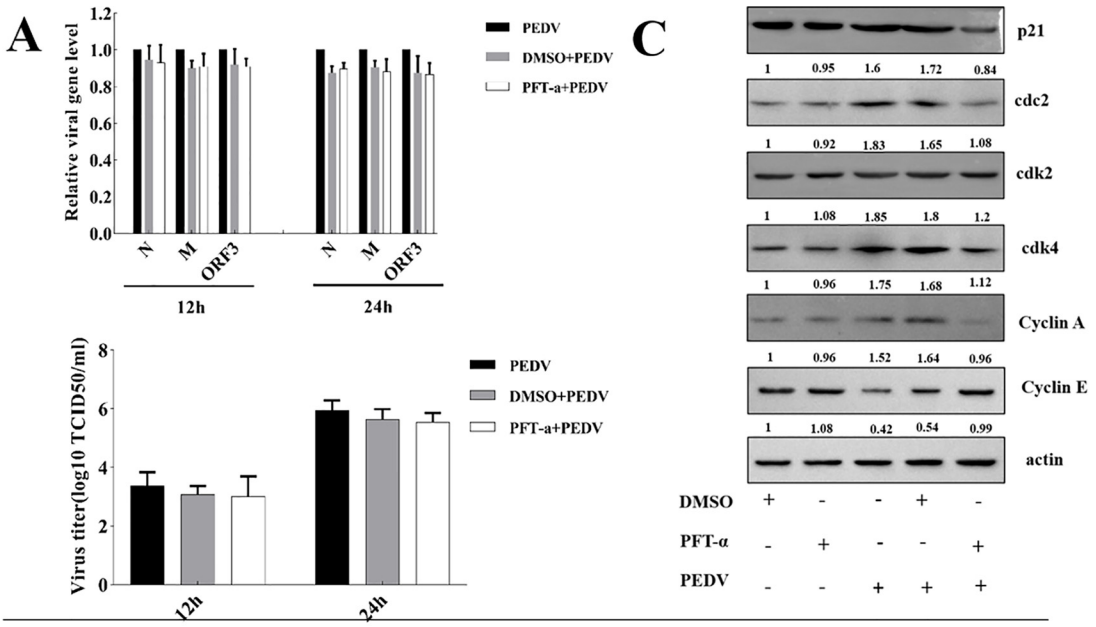

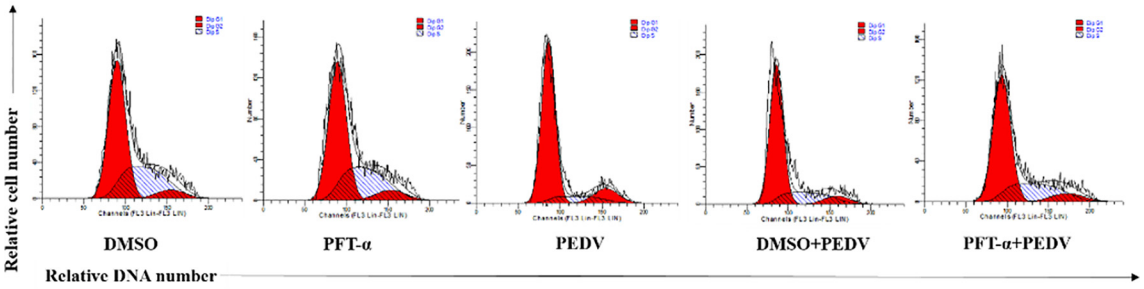

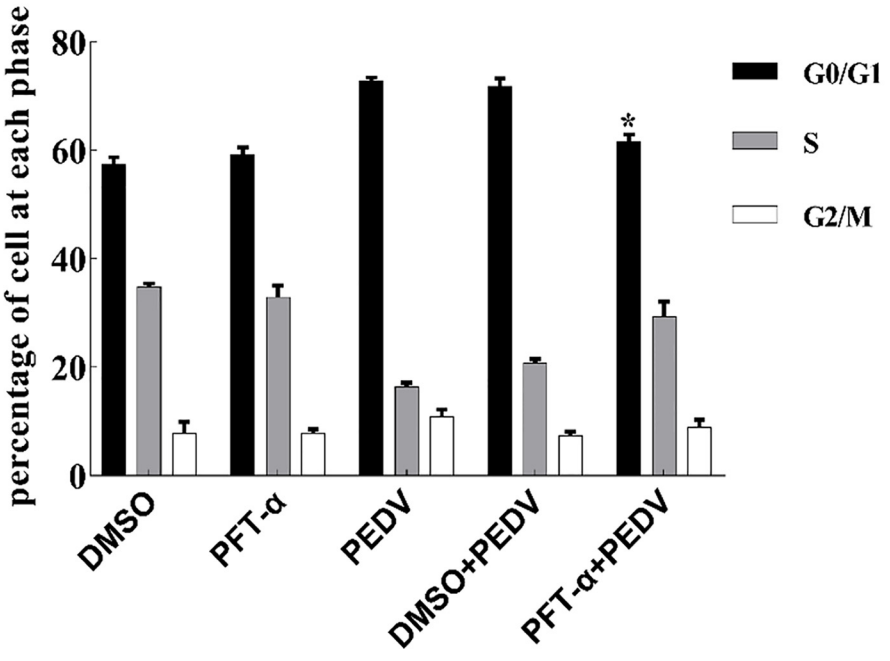

(caption on next page)

Fig. 8. Roles of p53 and p21 in PEDV-induced cell cycle arrest. (A) Effects of PFT-α (p53 inhibitor) on the transcription of PEDV sgmRNA levels of N, M, ORF3 and the titers of PEDV. Vero cells were pretreated with DMSO or PFT-α (10 μM) for 1 h and then infected with PEDV (0.5 MOI) for 1 h. After removal of the inoculum, the cells were continuously treated with DMSO or 10 μM PFT-α for 12 and 24 h. The relative PEDV genes mRNA levels were detected by quantitative real-time PCR (qRT-PCR), the titers of PEDV were detected by $TCID_{50}$. (B) Effects of PFT-α on the changes of cell cycle progression induced by PEDV infection. Vero cells were pretreated with PFT-α for 1 h, and then co-incubated with PEDV for 18 h. Cells were co-stained with BrdU and PI and analyzed by FACS analysis. The histograms were analyzed using the GraphPad Prism 7.0 software to determine the percentage of cells at each phase. (C) Effect of PFT-α on expression of p21, cdks and cyclins induced by PEDV infection. Cells were treated as in (B), and then collected and subjected to western blot analysis. The experiment was performed three. *P < 0.05, **P < 0.01 versus mock infection.

some viruses can regulate cell cycle progression through virus-cell interactions, thereby inducing cell cycle arrest and providing a favorable environment for viral replication (Dove et al., 2006; Ding et al., 2013). For example, TGEV, a coronavirus which can induce cell cycle arrest in a p53 dependent way, could increase protein accumulation and progeny virus production in cells enriched in both S and G2/M phases of cell cycle (Ding et al., 2013). PEDV and TGEV not only are coronavirus, but also induce cell cycle arrest in a p53 dependent way. In order to find out the biological significance of PEDV-induced cell cycle arrest and whether PEDV could increase protein accumulation and progeny virus production in cells enriched in G0/G1 phase similar to TGEV, we synchronized cells in various stages of cell cycle and compared their virus

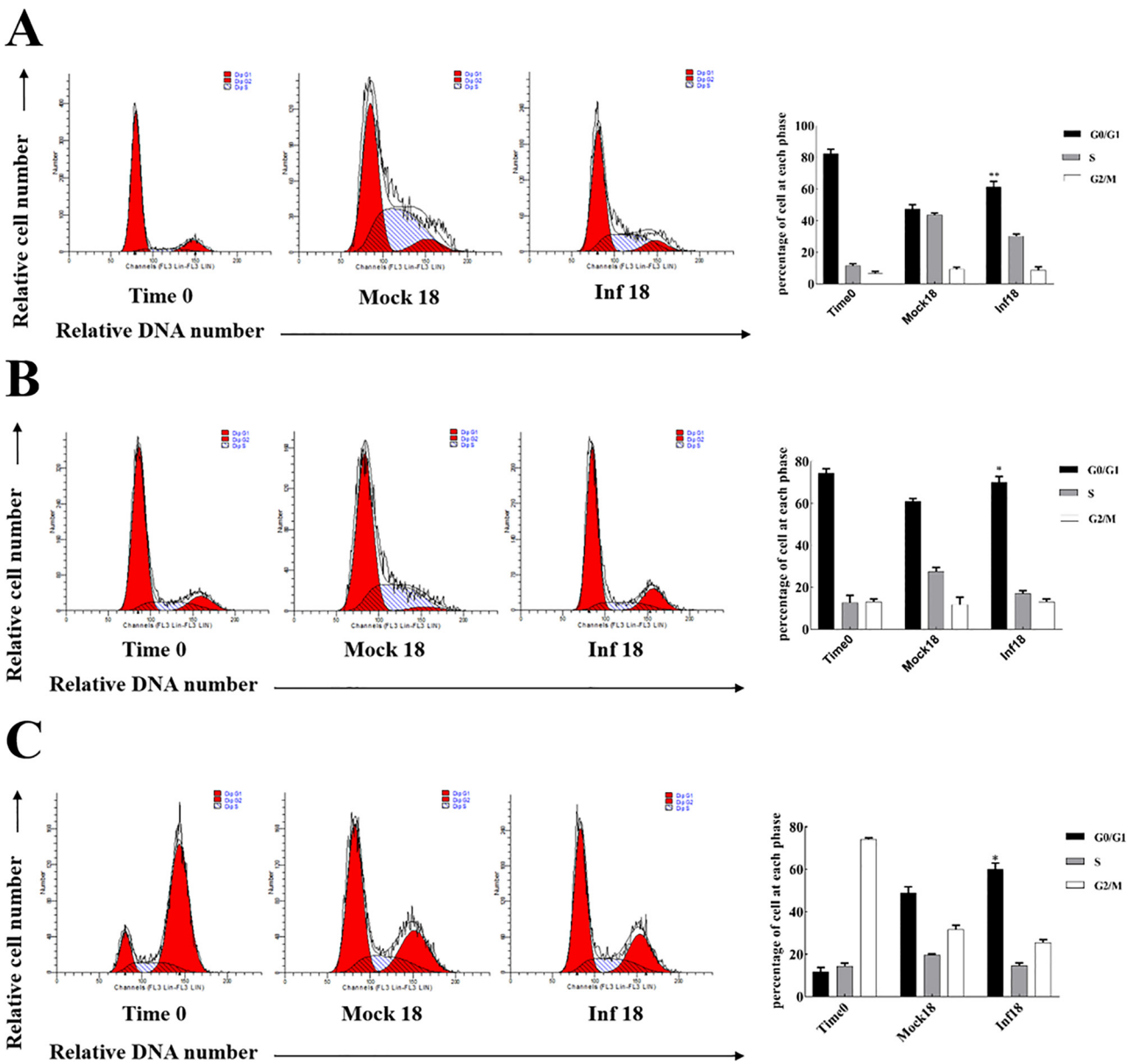

Fig. 9. G0/G1, G1/S and G2/M phases synchronization treatment. (A) Serum-starved Vero cells were mock infected or infected with PEDV. Cell cycle profiles at 18 h p.i. were determined by FACS analysis. (B) Cell cycle profiles of Vero cells synchronized at the G1/S phase border using double-thymidine treatment. Following synchronization (time 0) cells were released from block and simultaneously mock infected and infected with PEDV, and cell cycle profiles were analyzed at 18 h p.i.. (C) Asynchronously growing Vero cells were treated with nocodazole for 16 h. Following synchronization (time 0) cells were released from block and simultaneously mock-infected and infected with PEDV. Cell cycle profiles were analyzed at 18 h p.i.. The results are shown as mean ± SEM of three independent experiments. *$P < 0.05$, **$P < 0.01$ versus mock infection.

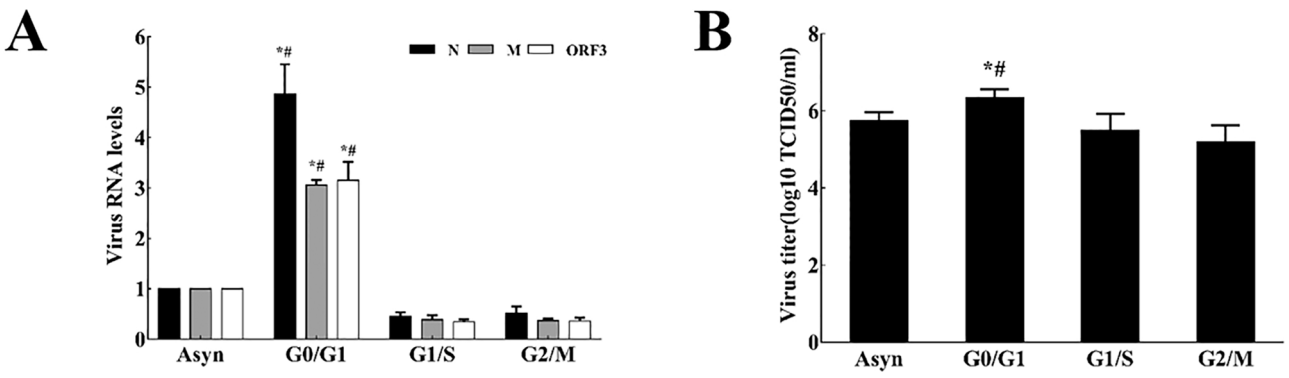

Fig. 10. Effects of cell cycle arrest at G0/G1 phase on PEDV replication. (A) PEDV sgmRNAs levels. PEDV sgmRNAs levels were determined at 18 h p.i. by RT-qPCR in the cells released from G0/G1, G1/S, G2/M-synchronized cells and asynchronous replicating cells. *$P < 0.05$ versus the RNA levels of PEDV in G1/S, G2/M-released cells. #$P < 0.05$ versus RNA levels of PEDV in asynchronous cells. (B) The titers of PEDV in different treated cells. Total virus at 18 h p.i. was harvested by freezing and thawing cells three times and the viral titers were shown as log10 $TCID_{50}$/ml. Values are shown as the mean ± SEM. *$P < 0.05$ versus the titer of PEDV in G1/S, G2/M-released cells. #$P < 0.05$ versus the titer of PEDV in asynchronous cells.

infection efficiencies. The results showed that PEDV sgmRNA synthesis were greater and PEDV titer was higher in the cells released from G0/G1 phase after 18 h p.i., when compared to either cells released from the S phase, G2/M phase or asynchronous cells. One possibility is that cell cycle arrest in G0/G1 phase provides increased amounts of ribonucleotide pool for efficient PEDV RNA synthesis. Since ribonucleotides are the precursors for synthesizing deoxyribonucleotides, a reduction in cellular DNA synthesis most likely increases the level of ribonucleotide pool in cells. Cell cycle arrest may also benefit PEDV replication in some other ways. Therefore, we favor the hypothesis that PEDV induces G0/G1 phase cell cycle arrest in order to provide a more favorable condition for virus production.

In conclusion, our study revealed that PEDV infection could induce G0/G1 phase arrest in both synchronous and asynchronous Vero cells, with up-regulations of p21, cdc2, cdk2, cdk4, Cyclin A protein and Cyclin E protein down-regulation. The G0/G1 phase arrest got reversed when p53 signaling pathway was inhibited, suggesting that PEDV through p53-dependent pathway causes cell cycle arrest in the G0/G1 phase, though more studies are required to verify whether or not this cell cycle arrest is cell type dependent. Moreover, the cell cycle arrest induced by PEDV infection might provide a more favorable condition for viral replication, since the cells released from G0/G1 phase were advantageous for PEDV replication.

Acknowledgements

This work was supported by grants from the state key laboratory of veterinary etiological biology (Grant No. SKLVEB2016KFKT003), the natural science foundation of Anhui Province (Grant No.1708085MC833) and the innovation project for agro-technology of Shaanxi Province (Grant No. 2016NY-095), China.

References

Besson, A., Dowdy, S.F., Roberts, J.M., 2008. CDK inhibitors: cell cycle regulators and beyond. Dev. Cell 14, 159–169.
Castedo, M., Perfettini, J.L., Roumier, T., Yakushijin, K., Horne, D., Medema, R., Kroemer, G., 2004. The cell cycle checkpoint kinase Chk2 is a negative regulator of mitotic catastrophe. Oncogene 23, 4353–4361.
Chen, C.J., Makino, S., 2004. Murine coronavirus replication induces cell cycle arrest in G0/G1 phase. J. Virol. 78, 5658–5669.
Chowdhury, I.H., Wang, X.F., Landau, N.R., Robb, M.L., Polonis, V.R., Birx, D.L., Kim, J.H., 2003. HIV-1 Vpr activates cell cycle inhibitor p21/Waf1/Cip1: a potential mechanism of G2/M cell cycle arrest. Virology 305, 371–377.
Davy, C., Doorbar, J., 2007. G2/M cell cycle arrest in the life cycle of viruses. Virology 368, 219–226.
Davidson, G., Niehrs, C., 2010. Emerging links between CDK cell cycle regulators and Wnt signaling. Trends Cell Biol. 20, 453–460.
De Bolle, L., Hatse, S., Verbeken, E., De Clercq, E., Naesens, L., 2004. Human herpesvirus 6 infection arrests cord blood mononuclear cells in G2 phase of the cell cycle. FEBS Lett. 560, 25–29.
Ding, L., Huang, Y., Dai, M.L., Zhao, X.M., Du, Q., Dong, F., Wang, L.L., Huo, R.C., Zhang, W.L., Xu, X.G., Tong, D.W., 2013. Transmissible gastroenteritis virus infection induces cell cycle arrest at S and G2/M phases via p53-dependent pathway. Virus Res. 178, 241–251.
Dove, B., Brooks, G., Bicknell, K., Wurm, T., Hiscox, J.A., 2006. Cell cycle perturbations induced by infection with the coronavirus infectious bronchitis virus and their effect on virus replication. J. Virol. 80, 4147–4156.
Duronio, R.J., 2012. Developing S-phase control. Genes Dev. 26, 746–750.
Elledge, S.J., 1996. Cell cycle checkpoints: preventing an identity crisis. Science 274, 1664–1672.
Enomoto, M., Goto, H., Tomono, Y., Kasahara, K., Tsujimura, K., Kiyono, T., Inagaki, M., 2009. Novel positive feedback loop between Cdk1 and Chk1 in the nucleus during G2/M transition. J. Biol. Chem. 284, 34223–34230.
He, Y., Xu, K., Keiner, B., Zhou, J., Czudai, V., Li, T., Chen, Z., Liu, J., Klenk, H.D., Shu, Y.L., 2010. Influenza A virus replication induces cell cycle arrest in G0/G1 phase. J. Virol. 84, 12832–12840.
Li, F.Q., Tam, J.P., Liu, D.X., 2007. Cell cycle arrest and apoptosis induced by the coronavirus infectious bronchitis virus in the absence of p53. Virology 365, 435–445.
Livak, K.J., Schmittgen, T.D., 2001. Analysis of relative gene expression data using real-time quantitative PCR and the $2^{-\Delta\Delta CT}$ method. Methods 25, 402–408.
Lundberg, A.S., Weinberg, R.A., 1998. Functional inactivation of the retinoblastoma protein requires sequential modification by at least two distinct cyclin-cdk complexes. Mol. Cell Biol. 18, 753–761.
Ma-Lauer, Y., Carbajo-Lozoya, J., Hein, M.Y., Müller, M.A., Deng, W., Lei, J., Meyer, B., Kusov, Y., von, Brunn B., Bairad, D.R., Hünten, S., Drosten, C., Hermeking, H., Leonhardt, H., Mann, M., Hilgenfeld, R., von, Brunn. A., 2016. p53 down-regulates SARS coronavirus replication and is targeted by the SARS-unique domain and PLpro via E3 ubiquitin ligase RCHY1. Proc. Natl. Acad. Sci. U. S. A. 113, E5192–201.
Pines, J., 1999. Four-dimensional control of the cell cycle. Nat. Cell Biol. 1, 73–79.
Poggioli, G.J., Keefer, C., Connolly, J.L., Dermody, T.S., Tyler, K.L., 2000. Reovirus-induced G2/M cell cycle arrest requires ç1s and occurs in the absence of apoptosis. J. Virol. 74, 9562–9570.
Reed, L.J., Muench, H., 1938. A simple method of estimating fifty per cent endpoints. Am. J. Epidemiol. 27, 493–497.
Roy, S., Gu, M., Ramasamy, K., Singh, R.P., Agarwal, C., Siriwardana, S., Sclafani, R.A., Agarwal, R., 2009. p21/Cip1 and p27/Kip1 are essential molecular targets of inositol hexaphosphate for its antitumor efficacy against prostate cancer. Cancer Res. 69, 1166.
Schlereth, K., Beinoraviciute-Kellner, R., Zeitlinger, M.K., Bretz, A.C., Sauer, M., Charles, J.P., Vogiatzi, F., Leich, E., Samans, B., Eilers, M., 2010. DNA binding cooperativity of p53 modulates the decision between cell-cycle arrest and apoptosis. Mol. Cell 38, 356–368.
Starostina, N.G., Kipreos, E.T., 2011. Multiple degradation pathways regulate versatile CIP/KIP CDK inhibitors. Trends Cell Biol. 22, 33–41.
Vogelstein, B., Lane, D., Levine, A.J., 2000. Surfing the p53 network. Nature 408, 307–310.
Weinberg, R.A., 1995. The retinoblastoma protein and cell cycle control. Cell 81, 323–330.
Xu, X.G., Zhang, H.L., Zhang, Q., Dong, J., Huang, Y., Tong, D.W., 2015. Porcine epidemic diarrhea virus M protein blocks cell cycle progression at S-phase and its subcellular localization in the porcine intestinal epithelial cells. Acta Virol. 59, 265–275.
Ye, S., Li, Z., Chen, F., Li, W., Guo, X., Hu, H., He, Q., 2015. Porcine epidemic diarrhea virus ORF3 gene prolongs S-phase, facilitates formation of vesicles and promotes the proliferation of attenuated PEDV. Virus Genes 51, 385–392.
Yuan, L., Chen, Z.B., Song, S.S., Wang, S., Tian, C.Y., Xing, G.C., Chen, X.J., Xiao, Z.X., He, F.C., Zhang, L.Q., 2015. p53 degradation by a coronavirus papain-like protease suppresses type I interferon signaling. J. Biol. Chem. 290, 3172–3182.
Yuan, X., Shan, Y., Zhao, Z., Chen, J., Cong, Y., 2005. G0/G1 arrest and apoptosis induced by SARS-CoV 3b protein in transfected cells. Virol. J. 2, 66.
Yuan, X., Wu, J., Shan, Y., Yao, Z., Dong, B., Chen, B., Zhao, Z., Wang, S., Chen, J., Cong, Y., 2006. SARS coronavirus 7a protein blocks cell cycle progression at G0/G1 phase via the cyclin D3/pRb pathway. Virology 346, 74–85.
Yuan, X., Yao, Z., Wu, J., Zhou, Y., Shan, Y., Dong, B., Zhao, Z., Hua, P., Chen, J., Cong, Y., 2007. G1 phase cell cycle arrest induced by SARSCoV 3a protein via the cyclin D3/pRb pathway. Am. J. Respir. Cell. Mol. Biol. 37, 9–19.